Supplementary methods for the mathematical model (S3):

The mathematical model developed is a compartment ODE model and is a variation of that developed by (Harrington et al., 2013). It is a phosphorylation and dephosphorylation system, with reactions following mass-action kinetics; however the shuttling reactions are not symmetric here (Fig. S3, A-C). Inhibitions along the pathway are studied to support the experimental findings in the main text. We use the Jacobian Injective Criterion to establish that this model in two compartments (cytoplasm and nucleus) is not injective and then determine parameter values from the Chemical Reaction Network Theory (CRNT) Toolbox, that provide bistability—a switch from one stable state to another, observed as two distinct responses. Often these distinct states are observed in mathematics using bifurcation diagrams (Fig. S3D), corresponding to dose-response curves in experimental science. This enables for different strengths or efficiencies of inhibitors to be studied. For example, the green curve shows that when FGF levels are low enough it results in the differentiation. Past this threshold level of FGF, the system undergoes proliferation. Similarly, the rate of ERK phosphorylation by Mek (k_3) results in differentiation under simulation settlings similar to that of UO126; however, as the rate of phosphorylation increases, the system hits a critical rate and the response switches so that differentiation can no longer occur. Finally, when studying the inhibition of ERK^{pp} translocation by EPE peptide, if the peptide decreases the shuttling rate, then this will always result in low nuclear ERK^{pp} (see red curve Fig S3D).

The compartment ODE model has 12 variables and 17 parameters describing the kinetic reactions and shuttling reactions (Fig S3, A-C). The presented model equations below describe the above reactions where subscript n denotes proteins in the nucleus, with conservation equations following.

$$[\dot{MEK}_n^{pp}] = -k_{13}[MEK_n^{pp}] + k_2[MEK_n^{pp}{+}ERK_n] + k_3[MEK_n^{pp}{+}ERK_n] - k_1[MEK_n^{pp}][ERK_n] + k_{16}[MEK^{pp}],$$

$$[\dot{MEK_n^{pp}{+}ERK_n}] = -k_2[MEK_n^{pp}{+}ERK_n] - k_3[MEK_n^{pp}{+}ERK_n] + k_1[MEK_n^{pp}][ERK_n],$$

$$[\dot{ERK}_n] = k_2[MEK_n^{pp}{+}ERK_n] - k_{14}[ERK_n] - k_1[MEK_n^{pp}][ERK_n] + k_6[F_n{+}ERK^{pp}{}_n],$$

$$[\dot{ERK}_n^{pp}] = k_3[MEK_n^{pp}{+}ERK_n] - k_{15}[ERK_n^{pp}] - k_4[ERK_n^{pp}][F_n] + k_5[F_n{+}ERK^{pp}{}_n] + k_{17}[ERK^{pp}],$$

$$[\dot{F}_n] = -k_4[ERK_n^{pp}][F_n] + k_5[F_n{+}ERK^{pp}{}_n] + k_6[F_n{+}ERK^{pp}{}_n],$$

$$[F_n{+}\dot{ERK^{pp}}{}_n] = k_4[ERK_n^{pp}][F_n] - k_5[F_n{+}ERK^{pp}{}_n] - k_6[F_n{+}ERK^{pp}{}_n],$$

$$[\dot{MEK}^{pp}] = k_{13}[MEK_n^{pp}] - k_{16}[MEK^{pp}] + k_8[MEK^{pp}{+}ERK] + k_9[MEK^{pp}{+}ERK] - k_7[MEK^{pp}][ERK],$$

$$[\dot{MEK^{pp}{+}ERK}] = -k_8[MEK^{pp}{+}ERK] - k_9[MEK^{pp}{+}ERK] + k_7[MEK^{pp}][ERK],$$

$$[\dot{ERK}] = k_{14}[ERK_n] + k_8[MEK^{pp}{+}ERK] - k_7[MEK^{pp}][ERK] + k_{12}[F{+}ERK^{pp}],$$

$$[\dot{ERK}^{pp}] = k_{15}[ERK_n^{pp}] + k_9[MEK^{pp}{+}ERK] - k_{17}[ERK^{pp}] - k_{10}[ERK^{pp}][F] + k_{11}[F{+}ERK^{pp}],$$

$$[\dot{F}] = -k_{10}[ERK^{pp}][F] + k_{11}[F{+}ERK^{pp}] + k_{12}[F{+}ERK^{pp}],$$

$$[F{+}\dot{ERK^{pp}}] = k_{10}[ERK^{pp}][F] - k_{11}[F{+}ERK^{pp}] - k_{12}[F{+}ERK^{pp}].$$

These conservation laws can be verified by adding the corresponding equations in the model. Since the model does not incorporate shuttling of the phosphatase, the amount of phosphatase is conserved separately in each compartment. We assume that the total activated MEK is proportional to the FGF signal. The differential equations in the conservation laws lead to the following equations that are fulfilled:

$$MEK_{tot}^{pp} = [\dot{MEK}_n^{pp}] + [\dot{MEK_n^{pp}{+}ERK_n}] + [\dot{MEK}^{pp}] + [\dot{MEK^{pp}{+}ERK}],$$

$$Fn_{tot} = [\dot{F}_n] + [F_n{+}\dot{ERK}^{pp}{}_n],$$

$$ERK_{tot} = [\dot{MEK_n^{pp}{+}ERK_n}] + [\dot{ERK}_n] + [\dot{ERK}_n^{pp}] + [F_n{+}\dot{ERK}^{pp}{}_n] + [\dot{MEK^{pp}{+}ERK}] + [\dot{ERK}] + [\dot{ERK}^{pp}] + [F{+}\dot{ERK}^{pp}],$$

$$F_{tot} = [\dot{F}] + [F{+}\dot{ERK}^{pp}].$$

1

A description of variables and parameters that were chosen within an order of magnitude of those reported in (Fukjioka J Biol Chem 2006, Harrington Phys Biol 2012) were found by using Latin Hypercube Sampling and satisfying bistability conditions.

k_1=0.012 $\mu M^{-1}s^{-1}$,
k_2=0.00172 s^{-1},
k_3=0.02419 $\mu M^{-1}s^{-1}$,
k_4=0.038 $\mu M^{-1}s^{-1}$,
k_5=0.0146 s^{-1},
k_6=0.0406 $\mu M^{-1}s^{-1}$,
k_7=0.0625 $\mu M^{-1}s^{-1}$,

k_8=0.0474 s^{-1},
k_9=0.00845 $\mu M^{-1}s^{-1}$,
k_{10}=0.0321 $\mu M^{-1}s^{-1}$,
k_{11}=0.0014 s^{-1},
k_{12}=0.00178 $\mu M^{-1}s^{-1}$,
k_{13}=0.01 s^{-1},
k_{14}=0.00058,
k_{15}=0.0015 s^{-1},

k_{16}=0.0096 s^{-1}, k_{17}=0.0013 s^{-1},
MEK_{tot}=1.4414 μM, Fn_{tot}=0.41068 μM, ERK_{tot}=97.1807 μM, Ftot=1.2301 μM.

In the main text (Fig 7C), the stimulus/inhibitors were included in the model by changes to the values of parameters/total amounts as follows: high FGF signal (MEKtot =2), SU5401 inhibition (MEKtot =1), UO126 (k3=0.006), EPE (k17=0.001)

2

Figure S1: **FGF signaling is reduced with the onset of myogenic differentiation in chick embryos**.

Analysis of FGF signaling during chick myogenesis (from stage 16 to stage 20) using whole-mount *in situ* hybridization for FGF ligands (**A**) and FGF target genes (**B**). White arrowheads indicate down-regulated genes in the area of the pharyngeal arches.

Figure S2: **Schematic representation of ERK2 and its nuclear translocation inhibitory peptide, EPE.** The nuclear translocation signal (NTS) of ERK, promotes its association with Importin7 and its translocation to the nucleus. The 18 mer EPE myristoylated (Myr) peptide fits to the kinase insertion domain (KID) of ERK2, in which the SPS sequence of ERK2 was changed to the phosphomimetic Glutamic acid residues forming EPE sequence instead. This peptide blocks the ERK-Importin interaction.

Figure S3: **ERK compartmentalization provides a bistable switch from proliferation to differentiation**

Dose response curves of the mathematical model. **A,B,** Simplified schematic of the model (FGF and its inhibitors). **C**, Full schematic of all enzymatic and translocation reactions. Gray lines are kinetic reactions, dashed lines are shuttling reactions. Depending on parameter values, the system can exhibit either a high or low nuclear ERK^{pp} state, or for regions of dashed lines, two response states, although this is a small region. **D**, Bifurcation diagrams (dose-response curves). Solid lines correspond to one response (low nuclear ERK^{pp} state (differentiation, colored) or high nuclear ERK^{pp} state (proliferation, black), dashed lines are the region when two responses can co-exist. Note that at low translocation rate of ERK^{pp} into the nucleus and at baseline (low) FGF levels, the system will always undergo differentiation.

Movie S1: Cytoplasmic expression of pERK in differentiating myoblasts (MHC+). Immunofluorescence of transverse sections of 4.5 days PMEE explants stained for DAPI, MHC and pERK. 3D imaging was obtained by a series of *z*-sections taken at 0.2 µm intervals. Image deconvolution was performed using Imaris (Bitplane).

Figure S1

A
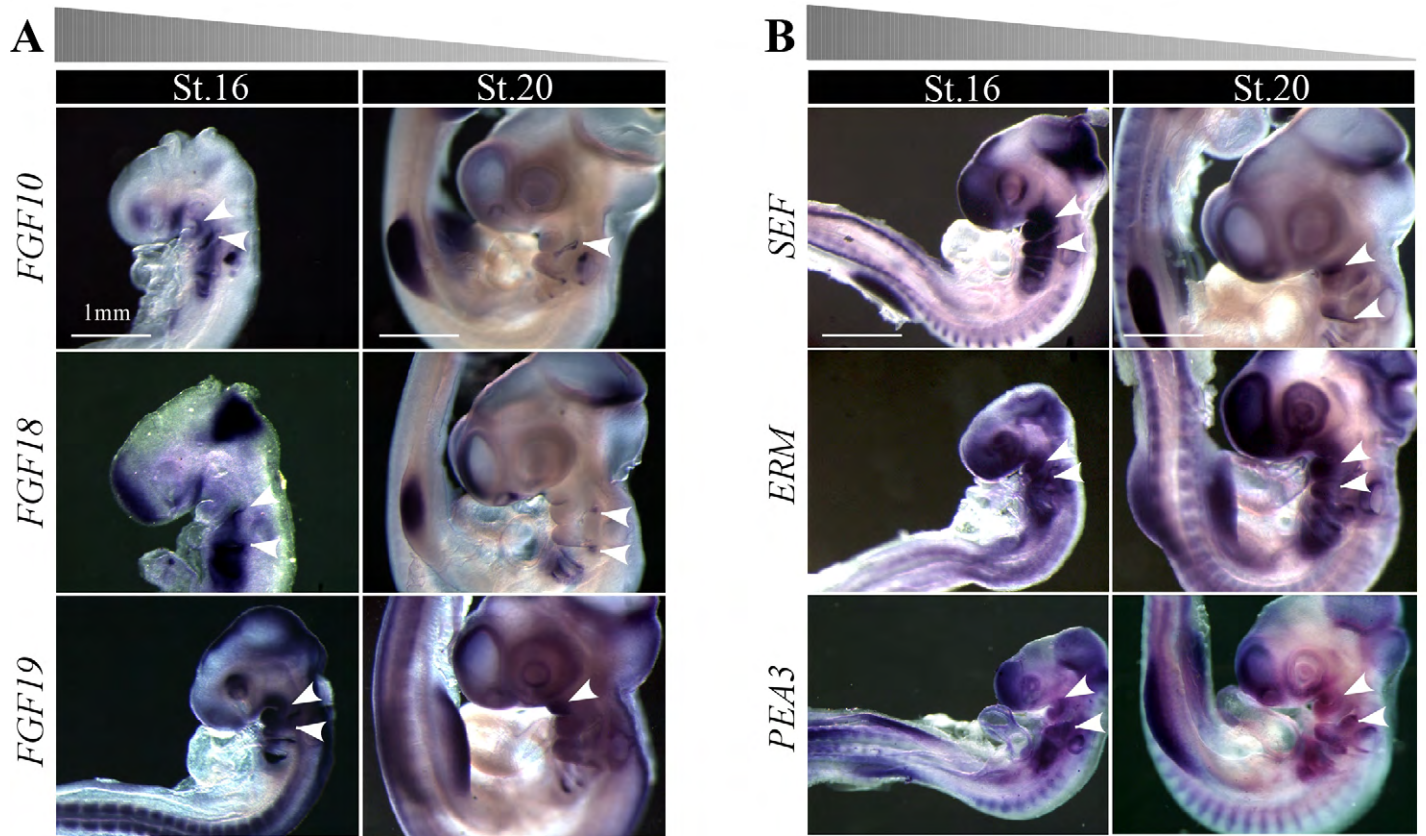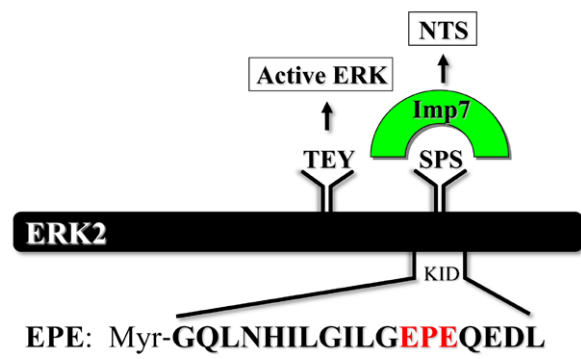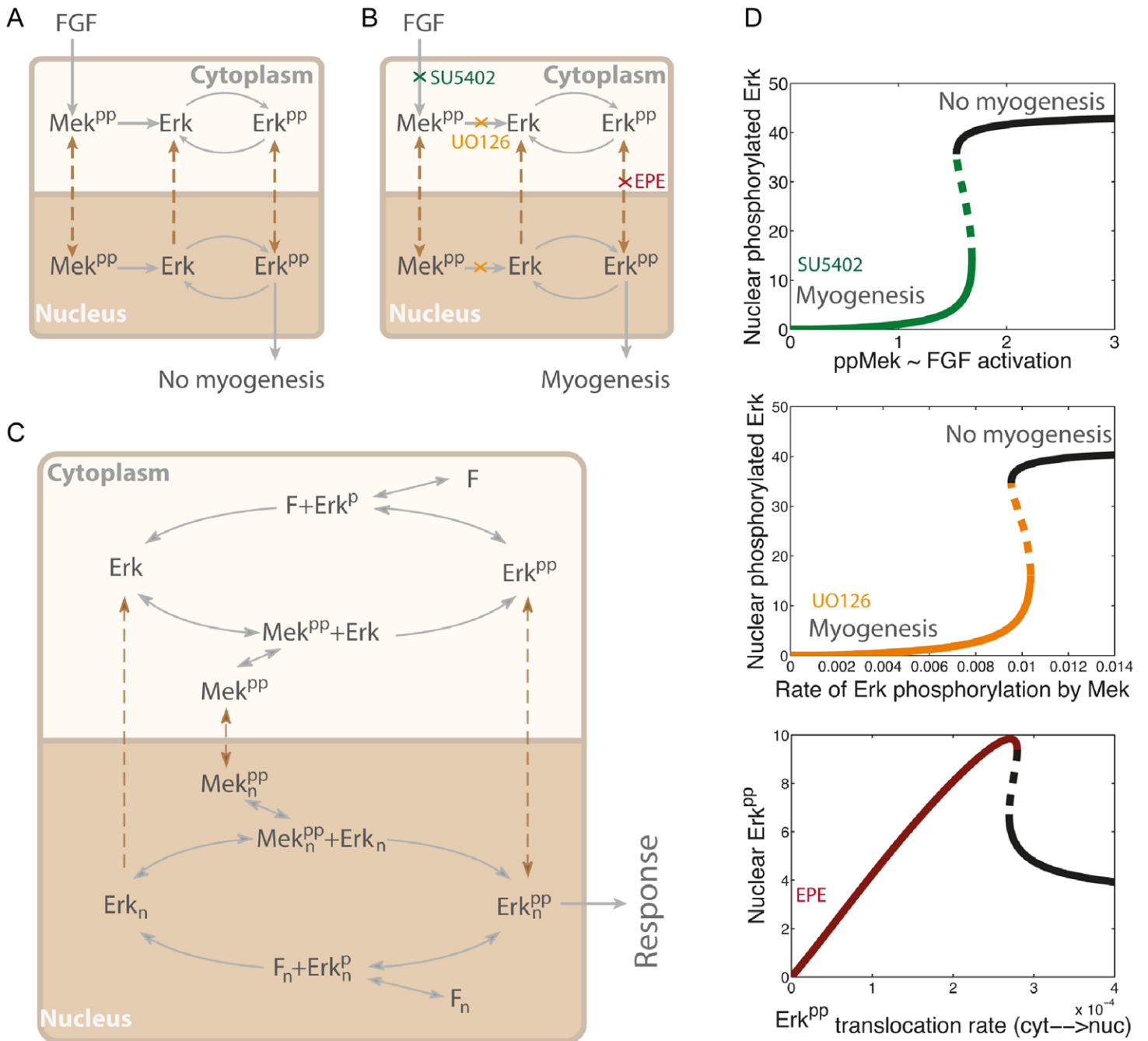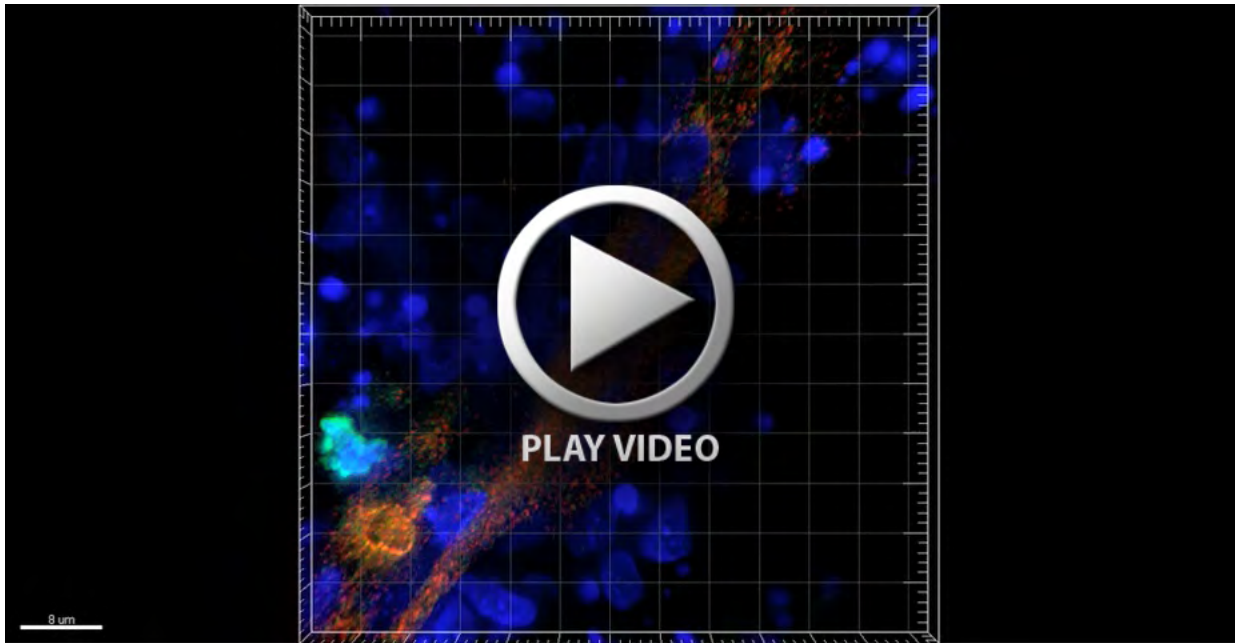
	St.16	St.20
FGF10		
FGF18		
FGF19		

1mm

B

	St.16	St.20
SEF		
ERM		
PEA3		

Figure S2

EPE: Myr-**GQLNHILGILGEPEQEDL**

Figure S3

Movie 1.

Table S1: a table of primer sequences for RT-PCR

Gene	Annealing Temp.	Forward primer sequence	Reverse primer sequence
Ccnd1	55	GTG GCT TCC AAA ATG AAG GA	CAG GAA AGG TCT GCT TCG TC
FGF10	50	AGC AAC TTC TGA GGC GAT CTG	GCC GTT CTT CTC GAT CTT GAG
FGF19	55	TTTCTCCCGCTGTCTCACTT	AATATGGCAACTGGGCACTC
FGF8	55	AGC AGA GCC TGG TGA CAG AT	CGG TTG AAG GGG TAG TTG AG
Frzb	60	TGG CAA CTG TAG AGG CAC TG	TTG CTG CTC CAA CAG TGA AG
GAPDH	60	AGT CAT CCC TGA GCT GAA TG	ACC ATC AAG TCC ACA ACA CG
MyoG	60	AGC CTC AAC CAG CAG GAG	TGC GCC AGC TCA GTT TTG GA
MHC	65	GAT CCA GCT GAG CCA TGC CA	GCT TCT GCT CAG CAT CAA CC
Myf5	55	CCC ATC CGA GCT CTT CTA TG	GAT GCT GGA GAG GCA GTC C
MyoD	60	GCA AGA GGA AGA CCA CCA AC	AAT CTG GGC TCC ACT GTC AC
Noggin	50	CGA CCC TAA CTT TAT GGC TAT	GGA CAG AGC AAG ACC TTT TAC
P21	55	CGGCTCCAAGAGAAGAGTTG	CAG TGA GGC TCT GAG GGT TC
PEA3	55	TGT GCC ACC TGA TCG TGT AT	CTG GGC AGA AGA GAA GGT TG
Slug	60	GCC AAA CTA CAG CGA ACT GG	GCA GTG AGG ACA GGA AAA CG
Sox9	60	AGG AAG CTG GCT GAC CAG TA	AGG TAC CGC TGT AGG TGG TG
Twist	60	CCG CAG TCC TAC GAG GAG CTG	GTG GGA TGC GGA CAT GGA CCA

Table S2: a table of primer sequences for qRT-PCR

Gene	Annealing Temp.	Forward primer sequence	Reverse primer sequence
Ccnd1	60	TAGTCGCCACTTGGATGCT	AGGGGAAAACTTCCTCTTCG
GAPDH	60	GGAGTCCACTGGTGTCTTCAC	GCTTAGCACCACCCTTCAGA
MyoD	60	ACTACACGGAATCACCAAATGA	GGAAATCCTCTCCACAATGC